Carbohydrate Research 344 (2009) 362–373

Contents lists available at ScienceDirect

Carbohydrate Research

journal homepage: www.elsevier.com/locate/carres

DFT conformation and energies of amylose fragments at atomic resolution. Part 1: syn forms of α-maltotetraose

Udo Schnupf [a], J. L. Willett [a], Wayne Bosma [b], Frank A. Momany [a,*]

[a] Plant Polymer Research, USDA,† ARS, National Center for Agricultural Utilization Research, 1815 N. University St., Peoria, IL 61604, USA
[b] Bradley University, Chemistry and Biochemistry Department, Peoria, IL 61625, USA

ARTICLE INFO

Article history:
Received 8 September 2008
Received in revised form 14 November 2008
Accepted 19 November 2008
Available online 9 December 2008

Keywords:
DFT
B3LYP/6-311++G**
DP-4 amylose
V-helix
COSMO

ABSTRACT

DFT optimization studies of 90 syn α-maltotetraose (DP-4) amylose fragments have been carried out at the B3LYP/6-311++G** level of theory. The DP-4 fragments studied include V-helix, tightly bent conformations, a boat, and a $^1C_4$ conformer. The standard hydroxymethyl rotamers (gg, gt, tg) were examined at different locations in the residue sequence, and their influence on the bridge conformations ϕ/ψ values and conformer energy is described. Hydroxyl groups were considered to be homodromic, that is, they are either in the all clockwise, 'c', or all counterclockwise, 'r'. Energy differences between conformations are examined in order to assess the stability of the different conformations and to identify the sources of energy that dictate amylose polymer formation. A small nearly cyclic compact structure is of low energy as one would expect when these flexible molecules are studied in vacuo. Many conformations in which the only differences are a single hydroxymethyl variation in the residue sequence show similar energies and bridge conformations, with trends being a result of the hydroxymethyl as well as hydroxyl orientation. In general the 'c' structures are of lower energy than the 'r' structures, although this is only true for the in vacuo state. The solvent dependence on conformational preference of several low-energy DP-4 structures was investigated via the continuum solvation method COSMO. These results suggest that the 'r' structures may be favored for fully solvated molecules.

Published by Elsevier Ltd.

1. Introduction

Starch is composed of two major fractions, linear amylose of α-(1→4)-linked glucose residues in the $^4C_1$-chair conformation, considered to be amorphous in starch, and the branched amylopectins, composed of two double helices with parallel strands linked at the 6-position, considered to be the more crystalline phase. Amylose conformations are generally denoted as A, B, and V-amylose types, with different configurations of water molecules and crystal orientations.[1–3] The dihedral angles at the glycosidic bonds determine the structural features, with the syn conformation being found in many carbohydrate structures. Recently,[4,5] larger structures have been found that contain anti conformations, that is, one glucose residue is flipped about the glycosidic bond dihedral angle ψ_H to a value of ~180°. These so-called 'band-flip' conformations are of interest because of the possible high-energy or stressed form related to such conformational transitions. Further, new structures[6,7] show 'kink' conformations, where adjacent residues in syn orientation are rotated out of the normal syn conformational state, but not flipped. These stressed conformations also require critical theoretical examination as to their stability. In particular, they appear to be the favored conformation of an amylose fragment bound at the active site of α-amylases.[6,7]

The carbohydrate α-maltotetraose is a four-glucose residue fragment of amylose, and it is of particular interest as it has nutritional and dietetic significance in enriched syrups.[8] It is also used as a diagnostic testing material for amylase enzymes.[9,10] In the work reported here, the syn form of α-maltotetraose becomes a model for larger amylose polymers.

Density functional geometry optimization studies at the B3LYP/6-311++G** level of theory have been carried out on more than 90 syn α-maltotetraose amylose fragments, denoted as DP-4s. This work is a continuation of an extensive computational study on carbohydrates from this laboratory that has, in particular, previously published the results of density functional theory (DFT) calculations for mono-,[11–16] di-,[17–23] and trisaccharides[24] in which the geometry, electronic energy, and conformational characteristics of these important carbohydrates have been obtained. DP-4 fragments are optimal for amylose studies as their structures are computationally accessible through DFT employing large basis sets, but they are sufficiently complex that one can begin to

* Corresponding author. Tel./fax: +1 309 681 6362.
E-mail address: frank.momany@ars.usda.gov (F.A. Momany).

† Names are necessary to report factually on available data; however, the USDA neither guarantees nor warrants the standard of the product, and the use of the name by USDA implies no approval of the product to the exclusion of others that may also be suitable.

0008-6215/$ - see front matter Published by Elsevier Ltd.
doi:10.1016/j.carres.2008.11.017

observe structural differences due to side-chain orientations and distance between end residues. To our knowledge, large basis set DFT structural/energetic studies of carbohydrates of this size and complexity have not been reported in the literature. Previously, the largest amylose-like structures that have been studied are DP-3 conformers.[24]

In the work presented here, we examine the $^4C_1$ ring conformations of DP-4 amylose fragments (four α-D-glucopyranose residues linked through the (1→4)-positions). These molecules have the possibility of great diversity in backbone conformations just by varying the hydroxymethyl groups to their gg, gt, or tg conformation (see Fig. 1). We report here structures in which each residue may have gg or gt hydroxymethyl conformations without regard to those groups on either side. The doubling of the number of conformers arises from the choice of either the clockwise 'c' or counterclockwise 'r' conformation for the hydroxyl groups (see Fig. 2). Thus, if all hydroxymethyl groups are denoted as gt–gt–gt–gt-c (the sequence is written from the non-reducing end (left) to the reducing end (right) and in this case 'c' denotes the hydroxyl groups are clockwise), we expect to find a particular set of ϕ_H/ψ_H values for each of the three bridging glycosidic regions. Changing the hydroxymethyl groups to gg–gg–gg–gg-c results in a different set of ϕ_H/ψ_H values and energy due to the different electronic surroundings throughout the molecule, resulting from the different orientations of the hydroxymethyl groups relative to one another. When different hydroxymethyl conformations on each successive residue are produced, such as the sequence gt–gg–gt–gg-c, one should find somewhat different ϕ_H/ψ_H values from those above. Changing all the hydroxyl groups to their 'r' orientation will give a totally different set of dihedral angles and energies for the examples described above. The higher energy tg conformers are not studied in such detail, although a number of tg-bearing conformations are examined, in particular, a very low energy conformation is found with residue *a* (non-reducing end) bearing a tg hydroxymethyl conformation.

Note that the starting conformation strongly influences the final optimized conformations of the DP-4 fragments. For example, if we create a very tight, almost cyclic structure, by using dihedral angles that are twisted away from the traditional maltose-like conformations, we find a very stable conformation of a tight nearly cyclic nature, stable simply because there is no solvent to act on the hydroxyl groups to allow the chains to extend back to normally observed forms (see Fig. 3). The very tight in vacuo conformation is of interest because of the strong electrostatic or hydrogen-bonding energy contributions, and would become less energetically favored if entropic contributions and solvent[15,16] were included. Of greater interest are those subtle differences in V-helix[3]-like and double-helix-like conformers when the hydroxymethyl groups are varied. These conformations will be examined in considerable detail. Band-flip and 'kink' forms are presented in Paper II of this series.[25]

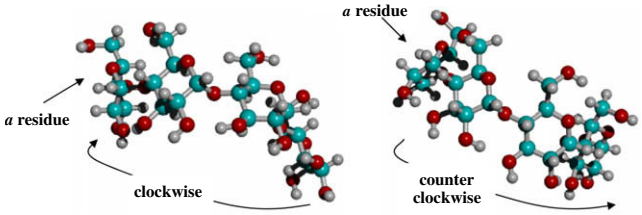

gg-gg-gt-gg-c *gg-gg-gt-gg-r*
'c' form *'r' form*
ΔE=0.1 kcal/mol *ΔE=2.7 kcal/mol*

Figure 2. B3LYP/6-311++G** geometry optimized DP-4 amylose displaying the 'c' and 'r' orientation of the hydroxyl groups.

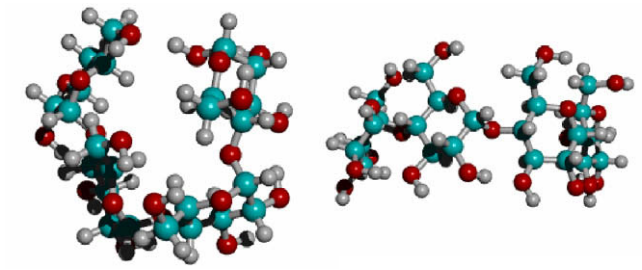

gt-gt-gt-gg-r *gt-gt-gt-gg-r*
sharp folded conformation *normal form*
ΔE=1.0 kcal/mol *ΔE=4.4 kcal/mol*

Figure 3. B3LYP/6-311++G** geometry optimized DP-4 amylose displaying the difference between the sharp folded form and normal form.

Utilizing DFT methods, and keeping the above considerations in mind, it is possible to examine different states of the DP-4 fragments and analyze the parameters produced including internal coordinates, hydrogen-bond distances, end-to-end distances and improper dihedral angles, conformations of the soft variables, dipole moments, and finally electronic energies.

2. Computational methodology

Starting conformations are generated using in-house empirical potentials, AMB06C (unpublished), and the InsightII/Discover graphics/computational software.[26] In order to obtain coverage of the many different conformations, we have chosen to include all of the possible combinations of the gg and gt hydroxymethyl groups for both the homodromic clockwise, 'c', and counterclockwise, 'r', hydroxyl groups. Only a few selected combinations of tg

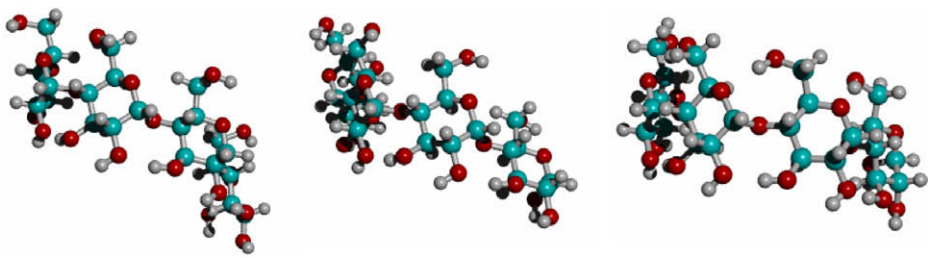

gg-gg-gg-gg-c *gt-gt-gt-gt-c* *tg-tg-tg-tg-c*
ΔE=0.3 kcal/mol *ΔE=3.7 kcal/mol* *ΔE=7.0 kcal/mol*

Figure 1. B3LYP/6-311++G** geometry optimized 'c' type DP-4 amylose fragments showing the different hydroymethyl orientations gg, gt, and tg.

conformational hydroxymethyl groups were examined, since tg is not found in X-ray studies of the dextran or cycloamylose fragments,[4,5] and it is found to be of higher energy than gg or gt conformers in monosaccharides[11–16] and maltose.[17–19]

DFT calculations are carried out using the B3LYP non-local exchange functionals with preliminary optimization using the 6-31+G* basis set, followed by optimization at the larger, 6-311++G**, basis set. This methodology has proven to be very useful for carbohydrates where hydrogen bonding is important for determining the conformational and structural parameters of these molecules. The smaller basis set is close to the larger basis set, but on occasions it is not sufficiently robust, in particular for molecules containing complex interactions of hydroxyl groups or those with explicit water.[15,16] Parallel Quantum Solutions[27] software and hardware (QS4-2000S, QS8-2600S, and QS16-2600S) were utilized

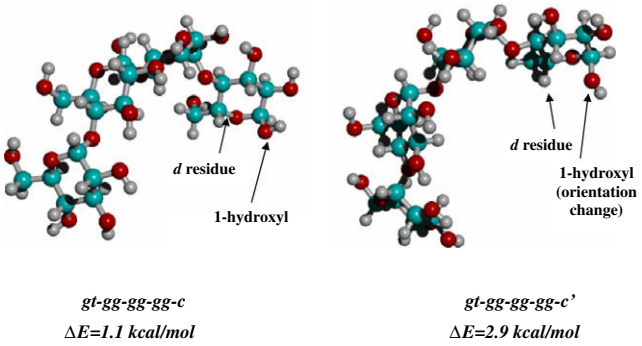

Figure 4. B3LYP/6-311++G** geometry optimized DP-4 amylose fragments showing the difference in the 1-hydroxyl and 2-hydroxyl orientation in the *d* residue.

Table 1
B3LYP/6-311++G** relative energies, conformations (ϕ_H/ψ_H dihedral angles in degrees) and dipole moments of 'r' type DP-4 amylose fragments

Conformer	Dihedral angles[a]						*ΔE* (kcal/mol)	Dipole (Debye)
	$\phi_{H1}{}^{ab}$	$\psi_{H4}{}^{ab}$	$\phi_{H1}{}^{bc}$	$\psi_{H4}{}^{bc}$	$\phi_{H1}{}^{cd}$	$\psi_{H4}{}^{cd}$		
All gg or single gt substitution								
gg–gg–gt–gg-c	−7.3	−17.9	−7.6	−17.7	−10.3	−16.2	0.1	4.0
gg–gt–gg–gg-c	−8.8	−19.7	−8.1	−17.3	−7.5	−16.5	0.3	5.6
gg–gg–gg–gg-c	−7.9	−20.4	−6.4	−18.6	−7.8	−20.9	0.3	3.9
gg–gg–gg–gt-c	−7.7	−19.6	−6.2	−16.6	−9.0	−21.8	0.5	2.4
gt–gg–gg–gg-c	−10.4	−18.0	−6.4	−18.5	−7.6	−19.9	1.1	5.7
gg–gg–gt–gg-c'[b]	−7.6	−18.3	−7.7	−18.8	−8.7	−17.0	1.9	4.9
gg–gg–gg–gt-c'	−7.7	−19.6	−6.2	−16.6	−7.7	−22.1	2.3	3.6
gt–gg–gg–gg-c'	−10.4	−18.1	−6.3	−18.5	−6.5	−18.5	2.9	7.2
Double substitutions								
gg–gt–gg–gt-c	−8.7	−20.3	−8.4	−17.4	−8.8	−22.0	0.5	4.3
gg–gt–gt–gg-c	−8.3	−19.6	−7.2	−21.3	−10.3	−15.3	0.9	6.1
gt–gg–gt–gg-c	−9.9	−18.3	−7.6	−19.3	−10.2	−16.3	0.9	5.6
gg–gg–gt–gt-c	−7.4	−18.6	−7.3	−19.7	−8.2	−24.9	1.2	3.6
gt–gg–gg–gt-c	−10.0	−18.3	−6.1	−16.7	−8.9	−21.7	1.3	4.0
gt–gt–gg–gg-c	−8.3	−23.9	−8.6	−17.0	−7.4	−18.4	2.0	7.2
gg–gt–gg–gt-c'	−8.8	−20.3	−8.4	−17.5	−7.6	−21.6	2.3	4.8
gg–gt–gt–gg-c'	−8.4	−19.8	−7.2	−21.7	−8.8	−16.0	2.7	6.5
gt–gg–gt–gg-c'	−10.1	−18.2	−7.5	−19.5	−8.6	−16.8	2.8	6.6
gg–gg–gt–gt-c'	−7.7	−18.7	−7.7	−20.9	−7.2	−25.2	2.9	3.5
gt–gg–gg–gt-c'	−10.1	−18.3	−6.0	−17.3	−7.6	−21.7	3.1	5.2
gt–gt–gg–gg-c'	−8.4	−23.9	−8.7	−17.0	−6.4	−17.7	3.8	8.3
All-gt or single gg substitution								
gg–gt–gt–gt-c	−8.2	−20.0	−6.7	−23.9	−8.3	−25.3	2.0	5.6
gt–gg–gt–gt-c	−9.8	−18.3	−7.0	−21.3	−8.1	−25.0	2.0	4.6
gt–gt–gg–gt-c	−8.1	−23.9	−8.4	−17.0	−8.8	−22.4	2.2	5.7
gt–gt–gt–gg-c	−7.7	−24.5	−7.2	−22.1	−10.2	−15.3	2.6	7.5
gt–gt–gt–gt-c	−7.6	−24.5	−6.9	−24.9	−8.2	−25.8	3.6	6.4
gg–gt–gt–gt-c'	−8.5	−20.2	−7.2	−24.6	−7.3	−25.9	3.6	5.3
gt–gg–gt–gt-c'	−10.1	−18.3	−7.4	−22.5	−7.2	−25.5	3.7	5.0
gt–gt–gg–gt-c'	−8.2	−24.0	−8.4	−17.1	−7.5	−22.0	3.9	6.4
gt–gt–gt–gg-c'	−7.8	−24.9	−7.2	−22.5	−8.7	−15.9	4.4	8.1
tg type								
tg–gg–gt–gg-c	−7.6	−19.7	−7.8	−18.3	−10.3	−15.8	**0.0**[c]	5.8
tg–gt–gg–gg-c	−8.8	−19.2	−8.5	−18.3	−7.4	−18.0	0.1	7.0
tg–gg–gg–gg-c	−7.9	−21.5	−6.7	−20.0	−7.7	−19.1	0.2	5.7
tg–gg–gg–gt-c	−7.9	−21.3	−6.5	−18.9	−8.8	−21.7	0.4	4.5
tg–gt–gg–gt-c	−8.8	−19.7	−8.5	−18.2	−8.8	−22.1	0.4	5.9
tg–gt–gt–gg-c	−8.2	−18.9	−7.2	−23.3	−10.3	−15.2	0.8	7.5
tg–gg–gt–gt-c	−7.9	−22.0	−7.4	−20.8	−8.2	−24.9	1.2	5.6
tg–gt–gt–gt-c	−8.3	−20.3	−7.0	−25.0	−8.1	−25.7	1.9	7.3
gg–gg–gg–tg-c	−7.5	−18.2	−6.5	−16.6	−6.9	−1.9	2.2	3.2
gt–gt–gt–tg-c	−7.8	−24.1	−8.8	−26.8	−7.9	7.9	5.4	6.5
tg–tg–tg–tg-c	−7.5	−2.5	−6.5	−3.7	−6.0	0.8	7.0	7.7
tg–tg–tg–tg-c'	−7.7	−3.1	−6.7	−5.5	−5.7	−0.7	8.3	7.7
$^1C_4$								
gg–gg–gt–gg-c'	−7.5	−19.8	−30.6	34.7	−26.1	14.3	14.9	2.0

[a] The dihedral angles are defined as follows: $\phi_{H1}{}^{ab}$ is H1a–C1a–O1a–C4b, whereas the superscripts label the ring starting from the non-reducing ring labeled as 'a'. $\psi_{H4}{}^{ab}$ is H4b–C4b–O1a–C1a. The other $\phi_H\psi_H$ dihedrals are defined analog just changing the ring labels.
[b] Conformations labeled with a ~-c indicate that the O1d–H hydroxyl group is pointing away from the hydrogen bonding net work toward the O5d ring oxygen.
[c] Electronic energy of the lowest energy 'c' conformer is −1581480.2 kcal/mol.

Table 2
B3LYP/6-311++G** relative energies, conformations (ϕ_H/ψ_H dihedral angles in degrees) and dipole moments of 'r' type DP-4 amylose fragments

Conformer	Dihedral angles[a]						ΔE[b] (kcal/mol)	Dipole (Debye)
	$\phi_{H1}{}^{ab}$	$\psi_{H4}{}^{ab}$	$\phi_{H1}{}^{bc}$	$\psi_{H4}{}^{bc}$	$\phi_{H1}{}^{cd}$	$\psi_{H4}{}^{cd}$		
Al- gg or single gt substitution								
gt–gg–gg–gg-r	−2.2	10.3	2.8	14.7	3.1	15.7	1.7	9.5
gg–gg–gg–gg-r	0.7	14.6	3.5	14.6	3.6	15.8	2.0	11.4
gg–gt–gg–gg-r	−3.8	12.9	−2.0	8.7	3.1	15.9	2.6	9.3
gg–gg–gt–gg-r	0.2	14.6	−3.8	11.0	−4.7	7.4	2.7	10.1
gg–gg–gg–gt-r	0.8	14.8	4.0	15.1	−3.6	13.1	3.0	11.6
gg–gg–gg–gg-r'[c]	0.4	14.6	2.6	13.9	2.9	15.6	5.2	13.1
Double substitutions								
gt–gg–gt–gg-r	−1.3	11.1	−2.8	12.6	−4.9	7.4	2.6	8.3
gt–gg–gg–gt-r	−0.4	11.8	4.8	15.7	−3.1	13.9	2.9	9.8
gt–gt–gg–gg-r	3.8	16.4	−2.5	8.4	1.9	15.4	2.9	7.5
gg–gt–gg–gt-r	−3.7	12.9	−1.7	9.2	−2.5	14.1	3.8	9.8
gg–gg–gt–gt-r	0.5	14.8	−3.6	11.1	2.6	14.7	4.4	10.9
gg–gt–gt–gg-r	−4.6	11.0	−11.6	14.3	−14.2	5.5	5.1	1.4
gt–gt–gg–gg-r''[d]	−8.2	−27.9	−0.7	9.8	3.1	16.1	3.1	9.0
gg–gt–gt–gg-r'''[e]	−5.3	10.3	−11.8	13.7	−14.5	4.9	8.5	3.5
All-gt or single gg substitution								
gt–gt–gg–gt-r	3.9	16.3	−1.0	9.9	−2.8	14.2	4.2	8.0
gt–gt–gt–gg-r	3.9	16.7	2.9	13.8	−5.3	7.3	4.4	6.5
gt–gg–gt–gt-r	−1.1	11.2	−2.2	12.9	2.6	14.9	4.4	9.2
gg–gt–gt–gt-r	−5.2	11.7	4.6	14.7	1.1	13.6	5.8	9.5
gt–gt–gt–gt-r	4.6	16.7	5.5	15.6	2.2	14.5	6.4	7.7
gt–gt–gg–gt-r''	−8.2	−28.3	−0.2	10.2	−2.8	13.9	4.3	9.7
gt–gt–gt–gg-r''	−8.2	−28.7	5.0	14.0	−2.9	9.7	4.6	8.1
gt–gt–gt–gt-r''	−8.5	−27.9	5.7	14.6	2.0	14.5	6.5	9.4
tg type								
tg–gg–gg–gg-r	2.4	16.6	3.6	15.3	3.3	15.9	1.8	9.4
tg–gt–gg–gg-r	−2.6	14.8	−2.6	8.5	2.8	16.0	2.6	7.7
tg–gg–gt–gg-r	2.7	16.9	−1.7	13.5	−4.4	8.3	2.6	8.1
tg–gg–gg–gt-r	2.1	16.6	3.5	15.3	−4.0	13.1	2.8	9.5
gg–gg–gg–tg-r	1.1	15.2	3.4	15.3	−0.5	13.5	3.3	11.0
tg–gt–gg–gt-r	−0.8	16.1	1.5	12.2	−3.2	14.1	3.9	8.1
tg–gt–gt–gg-r	−2.1	15.0	5.6	15.6	−5.2	7.5	4.0	6.6
tg–gg–gt–gt-r	3.7	17.4	−2.4	13.4	2.4	14.9	4.4	9.0
gt–gt–gt–tg-r	3.2	19.5	−16.2	31.7	−8.4	12.3	5.1	7.1
tg–gt–gt–gt-r	−1.9	15.3	6.4	16.0	2.9	15.0	6.0	7.9
tg–tg–tg–tg-r	2.1	15.8	3.5	15.6	1.9	16.5	6.9	6.3
tg–tg–tg–tg-r	1.7	15.4	1.4	14.7	−6.4	−36.4	9.4	9.0
tg–gt–gg–gg-r''	−10.5	−17.0	2.1	11.9	3.4	16.2	3.2	8.9
tg–gt–gg–gt-r''	−8.8	−26.1	3.6	12.4	−2.3	14.6	4.5	9.7
tg–gt–gt–gg-r''	−10.7	−16.5	7.5	15.5	−2.2	10.5	4.7	8.1
tg–gt–gt–gt-r''	−9.4	−26.1	7.0	15.3	3.4	15.7	6.6	9.7
Sharp folded conformation								
gt–gt–gt–gg-r	9.7	19.3	−39.0	58.0	−7.0	8.6	1.0	2.1
Boat								
gt–gt–tg–gg-r	21.1	16.5	−36.4	46.3	−30.0	21.4	15.2	2.9

[a] See Table 1 for definition of dihedral angles.
[b] See Table 1 for absolute value of lowest energy conformer.
[c] Conformations labeled with a ∼-r indicate that the O2–H hydrogen is rotated away from O1 but maintains the hydrogen bond with the O3–H hydroxyl group. This can occur on the reducing or first non-reducing ring or both.
[d] In this case the C1a–C2a–O2a–H has a dihedral angle of ∼(+25) instead of the typical dihedral of ∼(−40).
[e] Both of the O6–H of the gt conformations are pointing away from the O5 ring oxygen.

throughout, and results are reported only for the large basis set. Convergence criteria were similar to those used for the monosaccharides[11–16] with an energy change of less than 1×10^{-6} Hartree and a gradient of less than 3×10^{-4} a.u. Results have been displayed using HYPERCHEM 8.0.[28]

We define the hydroxyl groups to be homodromic, either clockwise designated 'c' relative to the numbered glucose ring starting at the anomeric carbon atom and counting clockwise around the ring, or counterclockwise, designated as 'r'. Both conformational states are examined in this work. Because of the extended hydrogen-bond network, we do not mix the 'c' and 'r' conformations, that is, they are maintained homodromic. The hydroxymethyl groups are started in the gg, gt, or tg conformation, using the standard nomenclature for hydroxymethyl rotation around the C5–C6 bond (i.e., the first term is relative to the ether ring O5 oxygen, while the second term is relative to atom C4). The orientation of the hydroxyl hydrogen on the O6 atom is taken to be that which points toward a potential hydrogen bond acceptor (g+, g−, t).[14]

2.1. Selecting starting conformations

All the glucose rings in DP-4 were taken to be in the $^4C_1$ chair conformation (with few exceptions), and different conformations were built using the InsightII/Discover program[26] and in-house empirical potentials (AMB06C) developed for carbohydrates by the authors. When a unique structure is found that is stable using the empirical potentials, the coordinates are transferred to the PQS programs for geometry optimization at the B3LYP/6-31+G* level of theory, and the structures resulting from this minimization are re-optimized at the B3LYP/6-311++G** level of theory. Only the re-

Table 3
Calculated[a] and experimental[b] dihedral angles, glycosidic angles, and virtual angles from the X-ray structure of cycloamylose, CA26[c,d] and maltotetraose

Dihedral angles[f]	X-ray[c]		X-ray[d]		Calculated values					
	ϕ	ψ	ϕ	ψ	ϕ^{ab}	ψ^{ab}	ϕ^{bc}	ψ^{bc}	ϕ^{cd}	ψ^{cd}
Max (helical)	115.3	131.4	112.1	127.1	'c' 109.6	115.3	110.7	114.2	110.7	125.2
					'r' 121.4	137.9	124.4	149.1	120.5	135.1
Min (helical)	91.1	97.4	89.6	99.7	'c' 106.7	95.5	108.4	95.5	106.8	94.3
					'r' 104.5	92.2	101.9	127.7	102.5	123.9
Mean (helical)	103.6	115.3	104.4	114.6	'c' 108.5	100.9	109.6	101.3	108.7	102.0
					'r' 114.7	125.2	117.6	132.3	115.6	130.5

Maltotetraose[e,g]	Type 1[e]		Type 2[e]		Ave[g]		Calculated[h]	
	ϕ	ψ	ϕ	ψ	ϕ	ψ	ϕ	ψ
Glc1-2	119.2	−100.4	125.9	−106.8	123.6	−103.5	'c' 108.5	−139.0
							'r'114.7	−114.6
Glc2-3	106.3	−124.0	91.6	−112.8	97.2	−119.5	'c'109.1	−138.6
							'r'118.9	−107.5

Glycosidic bond angle C(1)–O(1)–C(4) (degrees)	Calculated at central bonds, all gg/gt			
	X-ray[c]	X-ray[d]	'c'	'r'
Max	120.7	121.6	119.6	119.7
Min	114.6	114.6	117.6	117.0
Mean	118.3	118.0	118.1	118.9

Virtual angle O4–O4′–O4″ (degrees)	X-ray[c] Helical	Calculated for gg/gt	
		'c'	'r'
Max	136.7	136.2	142.1
Min	117.9	130.1	128.5
Mean	126.4	134.6	133.0

[a] Values calculated from vacuum conformations excluding special conformations such as mixed (c, r), $^1C_4$, sharp folded, and boat.
[b] Experimental values from Refs. 4–7.
[c] See Ref. 4.
[d] See Ref. 5.
[e] See Ref. 6.
[f] ϕ is defined as O5–C1–O1–C4′ and ψ is defined as C1–O1–C4′–C3′.
[g] See Ref. 7.
[h] ϕ is defined as O5–C1–O1–C4′ and ψ is defined as C1–O1–C4′–C5′.

sults from the larger basis set are included here. Implicit solvation calculations were carried out using COSMO[29] subroutines included in the PQS software.[27]

2.2. V-helix type structures

Numerous syn conformations similar to the V-helix type structures were studied. These conformers all appear to have overall curvature similar to that observed in a four-residue section of V-helix.[3] However, the side-chain differences create electronic disturbances that run throughout the molecule creating changes in bridging dihedral angles as well as minor variances in the dihedral angles of the 2- and 3-hydroxyl groups. On the non-reducing terminal-end residue *a*, the 4-position hydroxyl group is always taken to be in the same direction as the 2- and 3-position hydroxyls in that residue. Similarly, on residue *d* (reducing end), the 1-position hydroxyl is always taken to be in the same direction as the 2- and 3-position hydroxyls in that residue. One exception is in the 'c' form where the 1-hydroxyl group on the residue *d* can point toward the O5 ring oxygen instead of taking the same direction as the other hydroxyl groups (see top of Fig. 4). Further, the 2-hydroxyl group on the reducing end residue can take two conformations when in the 'r' form, one pointing the hydrogen atom directly toward the 1-hydroxyl axial oxygen atom, the second pointing 60° rotated away from the 1-position. Both conformations result in one lone-pair orbital pointing at the 3-hydroxyl hydrogen (see bottom of Fig. 4).

The conformational states of the hydroxymethyl groups are not always taken to be the same for each residue, and this allows for many possible configurations. Many conformations that could include a tg conformation are not studied, these being generally of high energy and entropy by both the empirical energy functions used in the molecular construction and from the resulting DFT energies of maltose[17,18] and DP-3 structures.[24] We also considered some experimental structures[4,5] using their conformational conditions as guides to important properties of DP-4 conformers. To this end it was observed that in the CA26 X-ray diffraction structures,[4,5] all the hydroxymethyl groups are either gg or gt with no tg conformers. Similarly, an α-maltotetraose molecule bound to α-amylase is of interest,[6,7] as is the molecule maltotritol,[30] where the 3-position hydroxyl group of the second residue points its hydrogen atom directly toward the O2 supporting the 'c' or clockwise hydroxyl groups direction, and giving us a direct ϕ_H/ψ_H comparison with our calculated values. A few examples of the tg conformation are examined, particularly on the 'a' residue position where this is a low-energy conformation. This case is suggestive of a form of end effect, which will be discussed later. However, tg hydroxymethyl conformations are generally of high energy in other positions in the chain, so the major concentration of this work is on the gg and gt forms.

3. Results

3.1. DP-4 conformations

In Tables 1–5 we list important conformational parameters and compare the calculated results with experimental data. Table 1 lists the 'c' type DP-4 conformers in order of their energy, and

Table 4
B3LYP/6-311++G** conformations of 'c' type DP-4 amylose fragments, dihedral angles (degrees) for the hydroxymethyl groups.

Conformer	Ring a		Ring b		Ring c		Ring d	
	OCCO[a]	CCOH[b]	OCCO	CCOH	OCCO	CCOH	OCCO	CCOH
Al- gg or single gt substitution								
gg–gg–gt–gg-c	−64.5	63.8	−59.3	60.3	65.1	−56.8	−62.2	61.6
gg–gt–gg–gg-c	−64.9	63.4	63.8	−58.0	−61.9	63.0	−57.9	58.0
gg–gg–gg–gg-c	−64.6	63.9	−59.2	60.9	−58.9	60.3	−58.1	58.1
gg–gg–gg–gt-c	−64.5	63.7	−59.1	60.8	−58.9	59.5	62.7	−51.5
gt–gg–gg–gg-c	63.6	−56.8	−63.3	64.8	−58.9	60.4	−58.0	58.0
gg–gg–gt–gg-c'[c]	−64.5	63.9	−59.3	60.3	64.0	−57.4	−61.4	59.0
gg–gg–gg–gt-c'	−64.5	63.8	−59.1	60.8	−58.8	59.1	61.1	−55.1
gt–gg–gg–gg-c'	63.7	−56.7	−63.3	64.7	−58.7	59.9	−58.1	56.2
Double substitutions								
gg–gt–gg–gt-c	−64.8	63.3	63.7	−57.8	−62.2	62.5	62.4	−51.4
gg–gt–gt–gg-c	−64.9	63.5	62.3	−57.1	63.5	−56.8	−62.2	61.9
gt–gg–gt–gg-c	63.1	−56.6	−63.1	63.9	64.7	−56.9	−62.1	61.7
gg–gg–gt–gt-c	−64.5	63.7	−59.3	60.3	62.4	−56.2	61.9	−51.4
gt–gg–gg–gt-c	63.3	−56.7	−62.9	64.3	−58.9	59.7	62.6	−51.5
gt–gt–gg–gg-c	60.9	−56.1	63.1	−57.9	−62.2	63.5	−58.0	58.1
gg–gt–gg–gt-c'	−64.8	63.4	63.8	−57.7	−62.1	62.1	60.8	−55.0
gg–gt–gt–gg-c'	−65.0	63.6	62.3	−57.1	62.5	−57.3	−61.5	59.3
gt–gg–gt–gg-c'	63.2	−56.6	−63.2	63.9	63.6	−57.5	−61.4	59.1
gg–gg–gt–gt-c'	−64.5	63.8	−59.3	60.2	62.0	−56.0	60.0	−54.8
gt–gg–gg–gt-c'	63.4	−56.7	−63.0	64.3	−58.9	59.3	61.0	−55.1
gt–gt–gg–gg-c'	61.0	−56.2	63.2	−57.9	−62.1	63.0	−58.0	56.3
All-gt or single gg substitution								
gg–gt–gt–gt-c	−64.9	63.3	61.9	−57.0	61.0	−55.7	62.0	−51.6
gt–gg–gt–gt-c	63.0	−56.7	−63.0	63.8	62.0	−56.1	61.9	−51.4
gt–gt–gg–gt-c	60.8	−56.0	62.7	−57.9	−62.2	62.8	62.4	−51.5
gt–gt–gt–gg-c	60.6	−56.1	61.2	−56.8	63.5	−57.1	−62.1	61.8
gt–gt–gt–gt-c	60.6	−56.1	60.9	−56.7	61.1	−56.0	62.0	−51.6
gg–gt–gt–gt-c'	−64.9	63.4	62.0	−56.8	60.9	−55.7	60.2	−55.1
gt–gg–gt–gt-c'	63.3	−56.7	−63.1	63.8	61.7	−56.0	60.1	−55.0
gt–gt–gg–gt-c'	60.8	−56.0	62.8	−57.8	−62.1	62.3	60.8	−55.1
gt–gt–gt–gg-c'	60.7	−56.1	61.3	−56.8	62.5	−57.6	−61.4	59.3
tg type								
tg–gg–gt–gg-c	−178.0	179.7	−59.0	59.6	64.6	−56.6	−62.2	61.8
tg–gt–gg–gg-c	−177.3	−178.3	63.8	−57.0	−62.0	63.1	−58.0	58.1
tg–gg–gg–gg-c	−178.0	179.5	−59.0	60.4	−58.7	60.1	−58.1	58.1
tg–gg–gg–gt-c	−178.1	179.7	−58.9	60.3	−58.8	59.4	62.5	−51.3
tg–gt–gg–gt-c	−177.5	−178.9	63.3	−57.0	−62.0	62.4	62.5	−51.3
tg–gt–gt–gg-c	−177.3	−178.7	61.8	−56.1	63.4	−56.7	−62.2	62.0
tg–gg–gt–gt-c	−178.1	179.5	−59.1	59.8	62.0	−55.8	61.8	−51.3
tg–gt–gt–gt-c	−177.4	−179.1	61.4	−56.1	61.0	−55.6	61.8	−51.4
gg–gg–gg–tg-c	−64.5	63.8	−59.1	61.0	−60.5	62.8	169.5	70.5
gt–gt–gt–tg-c	60.5	−55.8	59.7	−56.1	93.8	−56.9	171.0	66.5
tg–tg–tg–tg-c	−174.9	−169.8	169.9	68.8	169.7	69.8	167.9	71.3
tg–tg–tg–tg-c'	−175.0	−170.8	170.2	68.7	170.3	69.5	166.2	70.4
$^1C_4$								
gg–gg–gt–gg-c'	−64.2	63.1	−59.3	60.2	67.4	−71.1	−64.2	61.5

[a] OCCO is defined as O5–C5–C6–O6 at the specified ring.
[b] CCOH is defined as C5–C6–O6–H at the specified ring.
[c] See Table 1 for definition of c′.

presents the bridge dihedral angles as defined from atoms H1 and H4 at each bridge site, moving from left to right in the table as the sequence moves from the non-reducing end to the reducing end. The three sets of bridge dihedral angles define the total conformation of the four rings, and only the hydroxyl and hydroxymethyl groups remain to be defined. Table 2 shows the equivalent parameters as in Table 1 for the 'r' type DP-4 conformers. In Table 3 a comparison of the calculated results with experimental parameters shows that the calculated DP-4 results are in very good agreement with moderately high resolution X-ray data.[4,5] Tables 4 and 5 list the O5–C5–C6–O6 dihedral angles for the four hydroxymethyl groups including the C5–C6–O6–H6 dihedral angles which define the direction of the hydroxyl group for each hydroxymethyl. It can be seen in Tables 4 and 5 that the gauche (gt and gg) regions ($\chi_1 = +60^o$ and $\chi_1 = -60^o$) predominate in the choices for the heavy atoms of the hydroxymethyl groups, as they should, being of lower energy in general than the tg ($\chi_1 = 180^o$) region. It is important to note that for the more standard conformers (excluding for now those with tg conformations) there is not a great deal of deviation from the perfect threefold gauche positions.

3.2. Clockwise 'c' conformational energies

The lowest energy conformation (see Table 1) is the tg–gg–gt–gg-c structure with the structure, tg–gt–gg–gg-c, being ~0.1 kcal/mol higher in relative energy (ΔE). Examination of the all-gg sequences shows that addition of gt conformers to this series is somewhat unpredictable with regard to ΔE, where the energy difference changes from 0.5 kcal/mol for gg–gg–gg–gt-c, 0.1 kcal/mol for gg–gg–gt–gg-c, and 0.3 kcal/mol for the gg–gt–gg–gg-c structure, ending with 1.1 kcal/mol for the gt–gg–gg–gg-c conformer. There is little doubt that the all-gg-c conformer

Table 5
B3LYP/6-311++G** conformations of 'r' type DP-4 amylose fragments, dihedral angles (degrees) for the hydroxymethyl groups

Conformer	Ring a		Ring b		Ring c		Ring d	
	OCCO[a]	CCOH	OCCO	CCOH	OCCO	CCOH	OCCO	CCOH
All-gg or single gt substitution								
gt–gg–gg–gg-r	59.3	−61.2	−61.7	61.1	−61.9	61.5	−62.6	63.2
gg–gg–gg–gg-r	−57.5	56.1	−61.1	60.1	−61.9	61.5	−62.7	63.3
gg–gt–gg–gg-r	−58.1	57.3	60.3	−62.2	−62.5	62.5	−62.6	63.3
gg–gg–gt–gg-r	−57.6	56.4	−61.6	61.3	60.5	−63.3	−63.5	64.9
gg–gg–gg–gt-r	−57.5	56.2	−61.2	60.5	−62.7	63.0	63.0	−59.8
gg–gg–gg–gg-r'[b]	−57.4	56.0	−61.0	60.0	−61.7	61.3	−62.3	62.7
Double substitutions								
gt–gg–gt–gg-r	59.5	−61.3	−62.2	62.3	60.1	−63.0	−63.5	65.0
gt–gg–gg–gt-r	59.6	−61.0	−61.7	61.2	−62.8	63.1	62.8	−59.6
gt–gt–gg–gg-r	63.4	−59.7	59.1	−61.3	−62.6	62.8	−62.4	63.3
gg–gt–gg–gt-r	−58.1	57.5	60.3	−62.4	−63.1	64.2	62.6	−59.5
gg–gg–gt–gt-r	−57.7	56.6	−61.7	61.8	64.8	−62.4	61.3	−58.8
gg–gt–gt–gg-r	−57.9	55.6	74.8	−174.3	96.2	103.5	−81.0	−102.7
gt–gt–gg–gg-r″	60.7	−56.2	58.9	−62.2	−62.6	62.7	−62.6	63.3
gg–gt–gt–gg-r‴	−57.9	55.5	74.9	−173.9	96.1	104.0	−81.7	−102.5
All-gt or single gg substitution								
gt–gt–gg–gt-r	63.4	−59.7	59.2	−61.4	−63.2	64.2	62.5	−59.3
gt–gt–gt–gg-r	64.2	−59.7	62.7	−60.3	58.6	−62.0	−63.6	65.2
gt–gg–gt–gt-r	59.4	−61.2	−62.3	62.9	64.2	−62.1	61.1	−58.6
gg–gt–gt–gt-r	−58.2	58.0	65.1	−60.9	62.7	−61.9	60.6	−58.4
gt–gt–gt–gt-r	64.3	−59.6	63.7	−59.7	62.7	−61.3	60.7	−58.2
gt–gt–gg–gt-r″	60.6	−56.1	58.9	−62.3	−63.3	64.4	62.7	−59.6
gt–gt–gt–gg-r″	60.4	−56.1	62.5	−60.8	58.6	−62.2	−63.5	64.9
gt–gt–gt–gt-r″	60.4	−56.2	63.2	−60.8	62.5	−61.6	60.6	−58.3
tg type								
tg–gg–gg–gg-r	165.9	50.6	−61.2	60.2	−62.0	61.5	−62.6	63.2
tg–gt–gg–gg-r	166.3	50.4	59.5	−61.8	−62.5	62.7	−62.5	63.3
tg–gg–gt–gg-r	166.0	50.7	−61.9	61.6	60.1	−63.1	−63.5	64.9
tg–gg–gg–gt-r	165.9	50.6	−61.3	60.7	−62.6	62.9	62.9	−59.6
gg–gg–gg–tg-r	−57.6	56.2	−61.3	60.7	−64.0	66.3	159.4	74.9
tg–gt–gg–gt-r	166.4	50.5	59.8	−61.5	−63.1	63.9	62.6	−59.3
tg–gt–gt–gg-r	166.5	50.4	63.4	−60.2	58.9	−62.1	−63.6	65.1
tg–gg–gt–gt-r	166.1	50.7	−62.0	62.1	64.3	−62.1	61.2	−58.6
gt–gt–gt–tg-r	68.3	−57.1	82.3	−56.6	101.5	−56.8	167.2	71.0
tg–gt–gt–gt-r	166.6	50.4	64.2	−60.1	62.9	−61.2	60.9	−58.3
tg–tg–tg–tg-r	167.0	50.7	157.4	74.9	157.5	74.1	157.1	74.3
tg–tg–tg–tg-r	167.4	50.2	157.6	74.4	156.7	72.5	157.9	55.2
tg–gt–gg–gg-r″	166.4	50.2	59.1	−61.4	−62.6	62.5	−62.8	63.5
tg–gt–gg–gt-r″	166.4	50.2	59.3	−61.4	−63.3	64.1	62.5	−59.4
tg–gt–gt–gg-r″	166.5	50.0	63.0	−60.3	58.9	−62.2	−63.5	64.8
tg–gt–gt–gt-r″	166.5	50.1	63.2	−60.5	62.9	−61.3	60.9	−58.4
Sharp folded conformation								
gt–gt–gt–gg-r	66.1	−57.2	74.1	−69.1	73.3	−65.6	−60.4	60.5
Boat								
gt–gt–tg–gg-r	64.5	−55.3	60.7	−60.7	−168.9	83.1	−63.3	61.1

[a] See Table 4 for dihedral angle definitions.
[b] See Table 2 for definitions of r′, r″, and r‴.

is not significantly lower in energy than any single-site combination of gg and gt rotamers in the sequence. However, all-gg-c is lower in energy than any double substitution or single gg in an all-gt sequence. A similar energy series was found previously in our maltose[18] studies, where gg–gg-c is the lowest energy conformation, gg–gt-c is ∼0.4 kcal/mol higher in energy, and gt–gg-c is even higher at ∼3.2 kcal/mol, and gt–gt-c is ∼2.2 kcal/mol higher in energy.

It can be expected that within DP-4, long-range interactions play a significant role in the energetic contributions of the system, even though for the most part, the conformational differences in bridging dihedral angles are small between DP-4 and maltose.

In the paired substitutions such as gg–gg–gt–gt-c, a ΔE of ∼1.2 kcal/mol is found, ΔE of gg–gt–gt–gg-c is ∼0.9 kcal/mol, gt–gt–gg–gg-c is ∼2.0 kcal/mol, and gt–gg–gg–gt-c is ∼1.3 kcal/mol, suggesting that the end effects are modest but can lead to ∼1.0 kcal/mol of stabilization when gg comes before the pair of gt rotamers in the sequence. When the double substitution is split as in gg–gt–gg–gt-c, with a ΔE of ∼0.5 kcal/mol, the result is somewhat lower in energy than when paired substitutions are examined. The ΔE of gt–gg–gt–gg-c is ∼0.9 kcal/mol, somewhat higher in energy but not greatly different than above. Again, it depends on the positions of the different rotamers as to their energy preference, with gg at the non-reducing end being slightly preferred.

In the single gg-substituted all-gt-c conformer series, the ΔE of gg–gt–gt–gt-c is ∼2.0 kcal/mol, gt–gg–gt–gt-c ∼2.0 kcal/mol, gt–gt–gg–gt-c is ∼2.2 kcal/mol, and gt–gt–gt–gg-c is ∼2.6 kcal/mol higher in relative energy. The ΔEs of this series are somewhat paralleled by the dipole moments, the trend being 5.6 D, 5.0 D, 6.4 D, and 8.1 D, respectively. The gradual increase in ΔE as the gg conformation moves from the nonreducing to the reducing end of the DP-4 molecule is different and nearly opposite to the sequence observed above for gt moving through the all-gg-c sequence. The all-tg conformers are of high relative energy, and only tg at the

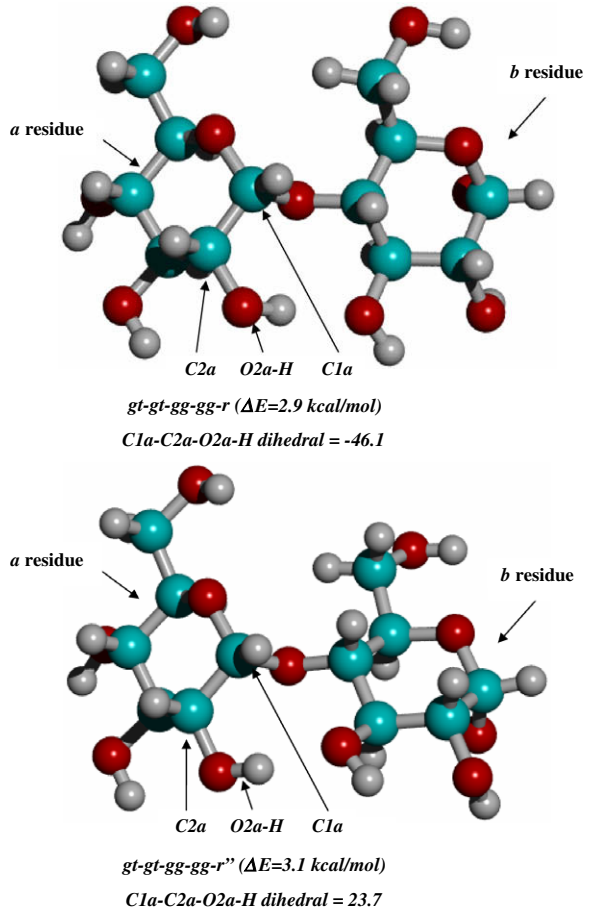

Figure 5. Difference between the *r* and *r*″ forms observed in the non-reducing end of the DP-4 amylose fragment. For clarification only the *a* and *b* residue is shown.

non-reducing end has interest because of its lowering of the relative energy.

3.3. Clockwise 'c' conformations

The ϕ_H^{bc}/ψ_H^{bc} values shown in Table 1 are generally similar for those structures in which gg hydroxymethyl forms predominate. Concentrating on the middle ϕ_H^{bc}/ψ_H^{bc} we find a considerable consistency, changing only as more gt conformations are included in a sequence, the average ψ_H^{bc} values increasing in magnitude in that case. The values for ψ_H^{cd} also show more variability with deviations of up to 5° from the ψ_H^{bc} values upon double substitution. The all-tg forms have very different conformations, with the ϕ_H values similar to the gg and gt forms, while the ψ_H values become much smaller.

3.4. Counterclockwise 'r' conformational energies

The lowest energy 'r' conformer ($\Delta E = \sim 1.0$ kcal/mol), which is denoted a 'sharp folded conformation' or gt–gt–gt–gg-r (see Table 2 and Fig. 3), is a structure distorted from the usual V-helix conformations and will be described later in this section. From Table 2 we see that the all-gg-r conformation is found to be higher in relative energy ($\Delta E = \sim 1.9$ kcal/mol) than the all-gg-c conformer. Replacing the nonreducing end gg with gt results in a structure with lower relative energy ($\Delta E = \sim 1.7$ kcal/mol). It was found that rotating the 2-hydroxyl group to point away from the 1-hydroxyl oxygen results in an energy loss of ~3.2 kcal/mol, leading to a stable conformation that retains its structure even after energy optimization. Replacing either of the middle gg residues with gt results in increasing the relative energy by ~0.6 kcal/mol. As found for the 'c' series, double substitutions increase the energy by several kcal/mol, the lowest energy double substitution being the gt–gg–gt–gg-r conformer with a ΔE of ~2.6 kcal/mol.

Several unusual sets of $\phi_H\psi_H$ values were found for the *a*–*b* bridge in several conformations, denoted with double primes in Table 2. In each case the hydroxymethyl sequence has two gt conformations, that is, gt–gt-X, and ϕ_H^{ab}/ψ_H^{ab} values of ~−8°/−28°. Structures of this case are shown in Figure 5. This unusual set of dihedral angles were examined by placing them at all three glycosidic positions in the starting conformation and carrying out energy optimization. In all cases, the structures returned to the conformations shown in Table 2. It appears that this conformational state is an end effect, again differentiating these larger structures from maltose, where this dihedral angle space is not an energy minimum.[19]

As noted above, the lowest energy conformation (gt–gt–gt–gg-r) in the 'r' series is a very tightly folded one in which the central bridging dihedral angles are considerably moved from the V-helix dihedral angles described for most conformers. In fact the ϕ_H^{bc}/ψ_H^{bc} values are more 'kink' than syn form. The resulting conformation is of low energy as a result of close hydrogen-bonding interactions, most of which would not be available in solution, and so this conformer is considered an anomaly and most probably unavailable experimentally. As already noted, this conformer is a very low energy 'r' conformation, being only ~1.0 kcal/mol higher in relative energy than the lowest energy 'c' conformer. Conformers in which at least one gg or gt-bearing residue (not in the *a* residue position) has been replaced with a tg are all of higher relative energy by ~5 kcal/mol or more and so would be of low probability, in agreement with experimental observations.

3.5. Conformations of 'r' forms

The 'r' conformational properties are also relatively consistent for the all-gg or one-gt substitution conformers, but the dihedral angles of the 'r' forms are found primarily in the (+, +) region of ϕ_H/ψ_H space relative to the (−, −) space of the 'c' forms as found for maltose,[18] and this is consistent with the ϕ_H/ψ_H isoenergetic maps of maltose.[19] As more gt forms are included in the sequence, the ψ_H values remain very much the same with smaller values of ϕ_H at all positions. The all-tg conformers are of interest since they do not show large variances in glycosidic dihedral angles from those sequences where the tg form is in the *a* residue position. The dipole moments of the 'r' forms are generally larger than those found for the 'c' forms.

3.6. Internal coordinates/structural parameters

In this section we report structural parameters of general interest including, hydrogen bond lengths, incremental structural differences between 'c' and 'r' conformers, and the effects of hydroxymethyl rotation upon close bonds and angles.

Tables 4 and 5 list the dihedral angles of the hydroxymethyl groups, O5–C5–C6–O6 and C5–C6–O6–H6 for the 'c' and 'r' forms, respectively. Only small deviations from the expected threefold rotamer positions are found, with variances of less than 5° being predominant. Some slight end effects can be found, for example, in the structure gg–gg–gg–gt-c, the *d* residue CCOH dihedral angle has a value of −51.5°, which is significantly different from that dihedral angle when found for gt conformers within the sequence. It also differs from the value when the 'c' form changes to the c-prime form, so it is responding to the conformational differences at the anomeric center. The *d* residue 'r' form (see Table 5) does

Table 6
B3LYP/6-311++G** conformations of 'c' type DP-4 amylose fragments, chain length, glycosidic bond angle, and virtual angles

Conformer	$O4^a$–$O4^d$ (Å)	$O1^a$–$O1^d$ (Å)	$C1^a$–$O1^a$–$C4^b$ (°)	$C1^b$–$O1^b$–$C4^c$ (°)	$C1^c$–$O1^c$–$C4^d$ (°)	$O4^a$–$O4^b$–$O4^c$ (°)	$O4^b$–$O4^c$–$O4^d$ (°)
All-gg or single gt substitution							
gg–gg–gt–gg-c	10.57	10.65	118.4	118.6	117.9	133.3	131.5
gg–gt–gg–gg-c	10.75	10.59	118.3	118.2	118.5	134.8	132.8
gg–gg–gg–gg-c	10.62	10.54	118.1	118.4	118.2	134.4	131.3
gg–gg–gg–gt-c	10.60	10.63	118.2	118.5	118.1	134.3	131.0
gt–gg–gg–gg-c	10.86	10.65	117.6	118.3	118.2	136.1	132.7
gg–gg–gt–gg-c'[a]	10.65	10.57	118.3	118.4	118.0	133.9	132.2
gg–gg–gg–gt-c'	10.57	10.47	118.2	118.5	118.1	134.3	130.8
gt–gg–gg–gg-c'	10.86	10.47	117.6	118.3	118.3	136.2	132.6
Double substitutions							
gg–gt–gg–gt-c	10.82	10.89	118.2	118.1	118.1	135.1	133.4
gg–gt–gt–gg-c	10.81	10.79	118.3	118.4	117.9	134.7	133.4
gt–gg–gt–gg-c	10.89	10.82	117.7	118.4	117.8	135.6	133.6
gg–gg–gt–gt-c	10.65	10.82	118.3	118.4	118.0	133.8	132.2
gt–gg–gg–gt-c	10.76	10.69	117.7	118.6	118.1	135.7	131.8
gt–gt–gg–gg-c	10.85	10.74	118.0	118.0	118.4	135.5	133.7
gg–gt–gg–gt-c'	10.83	10.75	118.2	118.0	118.1	135.3	133.6
gg–gt–gt–gg-c'	10.85	10.65	118.2	118.3	118.0	135.0	133.6
gt–gg–gt–gg-c'	10.91	10.67	117.7	118.4	118.0	135.9	133.6
gg–gg–gt–gt-c'	10.76	10.81	118.2	118.2	117.9	134.2	133.4
gt–gg–gg–gt-c'	10.78	10.56	117.7	118.5	118.1	135.8	131.8
gt–gt–gg–gg-c'	10.86	10.61	118.0	118.0	118.4	135.7	133.9
All-gt or single gg substitution							
gg–gt–gt–gt-c	10.83	10.93	118.3	118.3	118.0	134.7	133.6
gt–gg–gt–gt-c	10.88	10.92	117.8	118.4	118.0	135.5	133.5
gt–gt–gg–gt-c	10.78	10.88	118.1	118.1	118.1	135.1	133.2
gt–gt–gt–gg-c	10.86	10.82	118.1	118.3	117.9	135.1	133.9
gt–gt–gt–gt-c	10.85	10.98	118.1	118.2	118.0	134.8	134.1
gg–gt–gt–gt-c'	10.93	10.93	118.2	118.1	117.9	135.1	134.6
gt–gg–gt–gt-c'	10.99	10.91	117.7	118.1	117.9	136.0	134.6
gt–gt–gg–gt-c'	10.81	10.74	118.1	118.1	118.1	135.4	133.4
gt–gt–gt–gg-c'	10.92	10.70	118.0	118.2	118.1	135.6	134.3
tg type							
tg–gg–gt–gg-c	10.65	10.77	118.2	118.4	117.9	133.3	132.9
tg–gt–gg–gg-c	10.77	10.75	118.3	117.9	118.4	134.0	134.1
tg–gg–gg–gg-c	10.68	10.64	118.0	118.2	118.3	133.8	132.7
tg–gg–gg–gt-c	10.67	10.77	118.0	118.3	118.0	133.9	132.5
tg–gt–gg–gt-c	10.78	10.92	118.2	118.0	118.1	134.3	133.9
tg–gt–gt–gg-c	10.79	10.83	118.3	118.2	117.9	133.7	134.2
tg–gg–gt–gt-c	10.80	10.97	117.9	118.2	118.0	134.4	133.9
tg–gt–gt–gt-c	10.87	11.05	118.2	118.1	117.9	134.2	134.8
gg–gg–gg–tg-c	10.64	10.26	118.3	118.5	119.7	133.8	131.7
gt–gt–gt–tg-c	11.03	10.58	118.2	118.0	119.8	134.8	136.5
tg–tg–tg–tg-c	10.11	9.93	119.6	119.5	119.7	130.1	128.2
tg–tg–tg–tg-c'	10.11	9.76	119.5	119.4	119.6	130.1	128.2
$^1C_4$							
gg–gg–gt–gg-c'	7.85	9.19	118.2	117.5	117.7	134.1	91.9

[a] See Table 1 for definition of c'.

not appear to be so shifted, although other end effects can be found. Other significant differences occur within the tg forms where the CCOH values are significantly larger than 60°. In the all-tg forms, the *d* residue CCOH value depends upon the glycosidic bond difference, and moves from ~74° to ~55° a result of variation in ϕ_H^{cd}/ψ_H^{cd} values. The boat structure gt–gt–tg–gg-r also shows significant deviations in CCOH values at the *c* residue, but one expects this stressed form to show such differences.

The size of the DP-4 molecules allows us to get chain lengths for differing conformational states, and these are listed in Tables 6 and 7. The distance between atoms $O4^{a-d}$ or $O1^{a-d}$ of the syn 'c' conformers is listed in Table 6, and has a range of 10.5–10.9 Å, while for the 'r' conformers, listed in Table 7, the range is 9.7–10.9 Å. The exception to this range is found in the tightly folded conformation where the gt–gt–gt–gg-r fold brings the ends to within 8.2 Å in $O4^{a-d}$ distance and ~5.3 Å in $O1^{a-d}$ distance. The boat conformation also has very short end-to-end distances.

Glycosidic bond angles are also shown in Tables 6 and 7. From analysis of the X-ray structure of CA-26,[4,5] the glycosidic bonds averaged to 118.1° (see Table 3), which is in excellent agreement with our results shown in Table 6 for the 'c' conformers, while the 'r' syn conformers (see Table 7) give somewhat larger values, 118.9° on average. There appears to be no significant variation in the C1–O1–C4 angles resulting from the sequence position of different hydroxymethyl rotamers.

Calculated virtual angles, defined as $O4^a$–$O4^b$–$O4^c$, and similarly for *b*–*c*–*d* residues, are given in Tables 6 and 7. Table 3 lists some experimental and average calculated values for these parameters. The experimental and calculated values agree well for both the 'c' and 'r' forms, and therefore, one cannot use this parameter to predict hydroxyl directions along the chain, or for that matter, predict hydroxymethyl preferences.

One hydrogen bond length of interest is that interaction across the glycosidic bond (a detailed list can be found in the

Table 7
B3LYP/6-311++G** conformations of 'r' type DP-4 amylose fragments, chain length, glycosidic bond angle and virtual angles

Conformer	$O4^a$–$O4^d$ (Å)	$O1^a$–$O1^d$ (Å)	$C1^a$–$O1^a$–$C4^b$ (°)	$C1^b$–$O1^b$–$C4^c$ (°)	$C1^c$–$O1^c$–$C4^d$ (°)	$O4^a$–$O4^b$–$O4^c$ (°)	$O4^b$–$O4^c$–$O4^d$ (°)
All-gg or single gt substitution							
gt–gg–gg–gg-r	10.27	10.43	119.4	119.0	118.9	130.0	130.7
gg–gg–gg–gg-r	10.31	10.48	119.1	118.9	118.8	130.5	130.9
gg–gt–gg–gg-r	10.06	10.34	119.6	119.3	118.9	128.6	129.1
gg–gg–gt–gg-r	10.08	10.13	119.1	119.7	119.3	130.2	128.1
gg–gg–gg–gt-r	10.31	10.32	119.1	118.9	119.6	130.5	131.0
gg–gg–gg–gg-r'[a]	10.33	10.31	119.0	119.0	118.8	130.8	130.9
Double substitutions							
gt–gg–gt–gg-r	10.13	10.16	119.4	119.6	119.3	130.2	128.6
gt–gg–gg–gt-r	10.37	10.39	119.3	118.8	119.6	130.5	131.7
gt–gt–gg–gg-r	10.19	10.26	119.5	119.4	119.0	130.9	128.6
gg–gt–gg–gt-r	10.02	10.19	119.7	119.4	119.6	128.5	128.9
gg–gg–gt–gt-r	10.13	10.20	119.1	119.7	119.5	130.4	128.4
gg–gt–gt–gg-r	9.74	10.00	119.7	120.4	118.1	129.3	123.9
gt–gt–gg–gg-r'	10.91	10.42	117.2	119.3	118.9	140.7	130.0
gg–gt–gt–gg-r''	9.78	9.90	119.7	120.3	118.0	129.5	124.2
Al- gt or single gg substitution							
gt–gt–gg–gt-r	10.23	10.19	119.5	119.3	119.6	131.0	129.0
gt–gt–gt–gg-r	10.20	10.12	119.5	119.7	119.3	131.3	128.5
gt–gg–gt–gt-r	10.22	10.27	119.3	119.7	119.5	130.5	129.3
gg–gt–gt–gt-r	10.13	10.31	119.7	119.6	119.6	128.9	130.1
gt–gt–gt–gt-r	10.34	10.27	119.5	119.6	119.6	131.8	129.9
gt–gt–gg–gt-r'	10.93	10.31	117.1	119.2	119.6	140.8	130.3
gt–gt–gt–gg-r'	10.85	10.22	117.2	119.7	119.3	140.6	129.6
gt–gt–gt–gt-r'	10.97	10.37	117.2	119.5	119.6	141.0	130.8
tg type							
tg–gg–gg–gg-r	10.45	10.47	119.1	118.9	118.9	132.2	130.9
tg–gt–gg–gg-r	10.20	10.32	119.6	119.3	118.9	130.4	129.0
tg–gg–gt–gg-r	10.22	10.10	119.1	119.7	119.3	132.0	128.0
tg–gg–gg–gt-r	10.39	10.22	119.1	119.0	119.7	132.0	130.3
gg–gg–gg–tg-r	10.35	10.47	119.0	118.9	119.7	130.7	131.1
tg–gt–gg–gt-r	10.31	10.26	119.5	119.2	119.6	131.2	129.9
tg–gt–gt–gg-r	10.20	10.16	119.7	119.6	119.3	130.7	129.2
tg–gg–gt–gt-r	10.35	10.19	118.9	119.7	119.6	132.9	128.6
gt–gt–gt–tg-r	9.94	9.12	119.6	120.4	120.5	132.8	119.9
tg–gt–gt–gt-r	10.34	10.33	119.6	119.5	119.6	131.2	130.4
tg–tg–tg–tg-r	10.90	10.82	119.5	119.5	119.6	134.9	134.0
tg–tg–tg–tg-r	10.90	11.68	119.6	119.5	116.3	134.7	133.2
tg–gt–gg–gg-r'	10.78	10.42	117.8	119.3	118.8	138.2	130.1
tg–gt–gg–gt-r'	10.96	10.29	117.1	119.2	119.6	141.2	130.4
tg–gt–gt–gg-r'	10.80	10.31	117.8	119.5	119.3	138.3	130.6
tg–gt–gt–gt-r'	11.12	10.49	117.0	119.4	119.5	142.1	131.8
Sharp folded conformation							
gt–gt–gt–gg-r	8.19	5.25	119.5	121.0	122.1	132.9	90.7
Boat							
gt–gt–tg–gg-r	7.27	5.72	118.8	119.7	121.3	135.4	74.6

[a] See Table 2 for definitions for r′ and r″.

Table 8
COSMO-B3LYP/6-311++G** energies and conformations ($\phi_H\psi_H$ dihedral angles in degrees) of 'c' and 'r' type DP-4 amylose fragments

Conformer	Dihedral angles[a]						ΔE (kcal/mol)	Dipole (Debye)
	$\phi_{H1}{}^{ab}$	$\psi_{H4}{}^{ab}$	$\phi_{H1}{}^{bc}$	$\psi_{H4}{}^{bc}$	$\phi_{H1}{}^{cd}$	$\psi_{H4}{}^{cd}$		
All-gg								
gg–gg–gg–gg-c	−7.7	−3.6	−7.9	−3.3	−9.4	−8.7	1.7	4.1
gg–gg–gg–gg-r	−2.7	12.6	−4.5	10.6	−4.7	9.9	**0.0**[b]	12.6
All-gt								
gt–gt–gt–gt-c	−7.6	−11.7	−7.1	−8.7	−8.7	−11.3	2.2	8.9
gt–gt–gt–gt-r	−1.7	11.2	−2.7	−9.3	−3.6	8.5	1.6	8.7
All-tg								
tg–tg–tg–tg-c	−3.4	4.9	−2.2	6.3	−2.7	7.5	7.5	11.0
tg–tg–tg–tg-r	0.9	13.6	1.6	13.0	2.0	13.7	4.9	7.6

[a] See Table 1 for definition of dihedral angles.

Supplementary data) is formed between atoms O3 of one residue and O2 of a neighboring residue. An average value of 2.82 Å was found for the 'c' forms, while a value of 2.89 Å was found for the 'r' forms. The average calculated values fall into the range of the experimental values which range from 2.7 to 2.9 Å for the helical portions of the CA-26[4,5] X-ray structure.

Table 9
COSMO B3LYP/6-311++G** conformations of 'c' and 'r' type DP-4 amylose fragments, dihedral angles (degrees) for the hydroxymethyl groups, chain length, glycosidic bond angle, and virtual angles

Conformer	Ring a		Ring b		Ring c		Ring d	
	OCCO[a]	CCOH	OCCO	CCOH	OCCO	CCOH	OCCO	CCOH
All-gg								
gg–gg–gg–gg-c	−62.6	62.1	−60.8	61.7	−60.8	61.6	−60.4	61.5
gg–gg–gg–gg-r	−61.4	60.9	−61.9	62.0	−61.8	62.0	−61.7	61.9
All-gt								
gt–gt–gt–gt-c	63.5	−62.5	63.0	−62.5	62.9	−61.7	63.9	−58.6
gt–gt–gt–gt-r	63.1	−65.0	63.2	−65.8	62.7	−65.6	63.1	−58.6
All-tg								
tg–tg–tg–tg-c	178.4	169.1	160.9	72.7	160.3	72.8	162.1	72.5
tg–tg–tg–tg-r	166.7	50.7	155.8	74.8	156.3	74.2	158.3	74.0

Conformer	$O4^a$–$O4^d$ (Å)	$O1^a$–$O1^d$ (Å)	$C1^a$–$O1^a$–$C4^b$ (°)	$C1^b$–$O1^b$–$C4^c$ (°)	$C1^c$–$O1^c$–$C4^d$ (°)	$O4^a$–$O4^b$–$O4^c$ (°)	$O4^b$–$O4^c$–$O4^d$ (°)
All-gg							
gg–gg–gg–gg-c	10.12	10.28	119.0	118.9	118.6	129.8	129.0
gg–gg–gg–gg-r	10.14	10.16	119.2	119.2	119.2	129.8	129.2
All-gt							
gt–gt–gt–gt-c	10.29	10.42	118.8	118.9	118.6	131.1	129.9
gt–gt–gt–gt-r	9.96	10.04	119.5	119.5	119.4	128.8	127.8
All-tg							
tg–tg–tg–tg-c	10.20	10.19	119.4	119.4	119.4	130.2	129.1
tg–tg–tg–tg-r	10.86	10.47	117.6	118.3	118.3	136.2	132.6

[a] See Table 4 for dihedral angle definitions.

3.7. Implicit solvation

The effect of solvation on conformational and energetic preferences was investigated by introducing implicit solvation via the continuum solvation model COSMO.[29] Important structural and energetic information of the COSMO calculations are summarized in Table 8 and Table 9. Upon application of COSMO to selected DP-4 conformations obtained in vacuo, it is apparent that the energy preferences are reversed, now favoring the 'r' conformers over the 'c' forms, in the all-gg conformations by relative energy of ~1.7 kcal/mol. Interesting is the large difference in the all-gg-c/r dipole moments, from 4.1 D for 'c' versus 12.6 D for 'r'. As noted previously, the relative energy increases when going from all-gg to all-gt conformations, with the 'r' form remaining lower in energy than the 'c' form. The all-tg forms remain of higher energy with COSMO as they were in vacuo. A similar shift in favoring the full solvated 'r' form over the 'c' form was also observed in previous studies of maltose[18] and maltotriose.[24]

The energy difference between the c/r forms upon application of COSMO amounts to a relative change in energy of more than ~3.5 kcal/mol, and the glycosidic dihedral angles also change, more so with the 'c' conformer. The largest change is observed for the all-gg $\psi_{H4}{}^{ab,bc,cd}$ dihedral angles, changing upon inclusion of COSMO to smaller negative values by more than ~15°, whereas the change in the $\phi_{H1}{}^{ab,bc,cd}$ is much smaller. In the all-gt case, significant deviations in the resulting dihedral angles were also found upon optimization with the solvent model. Again in particular, changes were found in the $\psi_{H4}{}^{ab,bc,cd}$ values. Of interest is that the all-gt forms are of higher relative energy than the all-gg forms, suggesting that gg may be the favored hydroxymethyl conformation in solution. In the case of the all-tg forms, the conformers remain of relative high energy upon solvation compared to the all-gg and all-gt forms (~4–7 kcal/mol). In contrast to all-gg and -gt forms, the glycosidic dihedral angles show only very small variations upon addition of COSMO, suggesting that the tg forms have smaller allowed low-energy regions, which is in agreement with previous DFT mapping studies.[19]

It is of interest to directly compare our results with internal coordinates of the crystal structure of maltotritol.[30] Both hydroxymethyl groups are in the gt–gt conformation, and the direction of the hydroxyl groups is primarily of the 'c' form on the *a* residue. The $O5^a$–$C1^a$–$O1^a$–$C4^b$ dihedral angle was found to be 110.4° which compares to our 'c' mean value in Table 3 of 108.5°, while the measured $C1^a$–$O1^a$–$C4^b$–$C3^b$ value is 94.3 °, which compares favorably with our value 101.3°. Looking at our calculated 'r' values shown in Table 3, it is clear that one may be able under certain circumstances to use the dihedral angles associated with the X-ray structure to determine the secondary hydroxyl group's directionality around the ring. The calculated 'r' ϕ and ψ values of 132.3° and 130.5° are outside the range expected for the 'c' forms, but the decision remains difficult when the experimental values are in the minimum range of both 'c' and 'r' forms.

In Table 3 the mean (helical) calculated values for the cycloamylose, CA26, also suggest that the 'c' form has better fit to experiment.

4. Conclusions

Our conclusions regarding the syn forms of DP-4 follow those of our DP-3 results,[24] which suggested that maltose is not a particularly good model for larger starch fragments. In this work several end effects appear that make the two residues on each side of the central glycosidic bond appear to be ends of a chain, but with different conformational properties at the two ends. At first glance the syn forms studied here appear to be very similar in glycosidic dihedral angles even when moving from 'c' to 'r' hydroxyl directions, but one must remember that when larger systems are investigated, small differences in dihedral angles can make large changes in the positions of residues remote to the starting site. We do see differences in the overall conformations with small differences, and they are subtle to the point that figures become less illuminating unless they are extended to larger systems.

We have, as previously for the DP-3 examples,[24] examined a few solvated conformations and find that the application of an implicit solvent method, COSMO, results in changes in both relative energies, as well as conformational state. Although data are being gathered relative to the solvation question, it is premature to speculate as to the predictive ability of these implicit solvation models.

At the current level of theory and computing hardware, addition of explicit water molecules to many conformations of DP-4 creates a major hurdle to overcome, and only in the future may this become feasible. On the other hand, our previous explicit water studies[15,16] with one and five water molecules, respectively, around glucose, support the 'r' orientation found here. The few 'c' forms reported in those papers were all of very high relative energy. To date the computational evidence gained from our DFT with explicit water and DFT/COSMO calculations both point to the 'r' hydroxyl direction being favored in the fully solvated state. This result appears to be in agreement with solvation studies of Kirschner and Woods,[31] where the 'r' form was used in their explicit solvent empirical dynamics simulations, although their work is directed toward understanding the effect of solvent on the hydroxymethyl rotamer population (see also the solvation studies of reference[32]), and not on the orientation preference of the secondary hydroxyl groups.

In our search for low-energy conformational states to add to our list of favored structures on which to build larger fragments of amylose, the syn forms presented here are now well established with differences from maltose when moving to larger fragments. In Paper II of this series,[25] we present studies on several other conformational forms (i.e., 'band-flips' and 'kinks') which we add to our arsenal of starting conformations for carbohydrates. Our goal is to establish a library of favored conformations similar to those noted for proteins, recognizing that carbohydrates do not take on organized secondary structural motifs as strongly as do proteins, a result of broad and flat energy landscapes around the glycosidic bonds.[14]

Supplementary data

Supplementary data associated with this article can be found, in the online version, at doi:10.1016/j.carres.2008.11.017.

References

1. Sarko, A.; Zugenmaier, P. In *Fiber Diffraction Methods*; French, A. D., Gardner, K. C. H., Eds.; ACS Symposium Series; Am. Chem. Soc.: Washington, DC, 1980; Vol. 141, pp 459–482.
2. French, D. *Starch: Chemistry and Technology*, 2nd ed.; Academic Press: New York, 1984.
3. Rao, V. S. R.; Qasba, P. K.; Balaji, P. V.; Chandrasekaran, R. *Conformation of Carbohydrates*; Harwood Academic: Melbourne, 1998.
4. Gessler, K.; Uson, I.; Takaha, T.; Krauss, N.; Smith, S. M.; Okada, S.; Sheldrick, G. M.; Saenger, W. *Proc. Natl. Acad. Sci. U.S.A.* **1999**, *96*, 4246–4251.
5. Nimz, O.; Gebler, K.; Uson, I.; Saenger, W. *Carbohydr. Res.* **2001**, *336*, 141–153.
6. Yoshioka, Y.; Hasegawa, K.; Matsuura, Y.; Katsube, Y.; Kubota, M. *J. Mol. Biol.* **1997**, *271*, 619–628.
7. Hasegawa, K.; Kubota, M.; Matsuura, Y. *Prot. Eng.* **1999**, *12*, 819–824.
8. Kimura, T.; Nakakuki, T. *Starch/Stärke* **2006**, *42*, 151–157.
9. Whitlow, K. J.; Gochman, N.; Forrester, R. L.; Wataji, L. *J. Clin. Chem.* **1979**, *25*, 481–483.
10. Huang, G.-L.; Zhang, H.-C.; Wang, P.-G. *Food Chem.* **2007**, *101*, 392–396.
11. Appell, M.; Strati, G. L.; Willett, J. L.; Momany, F. A. *Carbohydr. Res.* **2004**, *339*, 537–551.
12. Momany, F. A.; Appell, M.; Willett, J. L.; Schnupf, U.; Bosma, W. B. *Carbohydr. Res.* **2006**, *341*, 525–537.
13. Appell, M.; Willett, J. L.; Momany, F. A. *Carbohydr. Res.* **2005**, *340*, 459–468.
14. Schnupf, U.; Willett, J. L.; Bosma, W. B.; Momany, F. A. *Carbohydr. Res.* **2007**, *342*, 196–216.
15. Momany, F. A.; Appell, M.; Willett, J. L.; Bosma, W. B. *Carbohydr. Res.* **2005**, *340*, 1638–1655.
16. Momany, F. A.; Appell, M.; Strati, G. L.; Willett, J. L. *Carbohydr. Res.* **2004**, *339*, 553–567.
17. Momany, F. A.; Willett, J. L. *J. Comput. Chem.* **2000**, *21*, 1204–1219.
18. Momany, F. A.; Schnupf, U.; Willett, J. L.; Bosma, W. B. *Struct. Chem.* **2007**, *18*, 611–632.
19. Schnupf, U.; Willett, J. L.; Bosma, W. B.; Momany, F. A. *Carbohydr. Res.* **2007**, *342*, 2270–2285.
20. Strati, G. L.; Willett, J. L.; Momany, F. A. *Carbohydr. Res.* **2002**, *337*, 1833–1849.
21. Strati, G. L.; Willett, J. L.; Momany, F. A. *Carbohydr. Res.* **2002**, *337*, 1851–1859.
22. Bosma, W. B.; Appell, M.; Willett, J. L.; Momany, F. A. *J. Mol. Struct.: THEOCHEM.* **2006**, *776*, 1–19.
23. Bosma, W. B.; Appell, M.; Willett, J. L.; Momany, F. A. *J. Mol. Struct.: THEOCHEM.* **2006**, *776*, 13–24.
24. Schnupf, U.; Willett, J. L.; Bosma, W. B.; Momany, F. A. *J. Comput. Chem.* **2008**, *29*, 1103–1112.
25. Paper II of this series, see accompanying paper.
26. InsightII/Discover, Accelrys Corp., San Diego, CA, USA.
27. PQS Ab Initio Program Package, Parallel Quantum Solutions, Fayetteville, AR, USA.
28. HYPERCHEM 8.0, Hypercube, Gainesville, FL, USA.
29. Klamt, A.; Schuurmann, G. *J. Chem. Soc., Perkin Trans. 2* **1993**, *5*, 799–805; Baldridge, K.; Klamt, A. *J. Chem. Phys.* **1997**, *106*, 6622–6633.
30. Schouten, A.; Kanters, J. A.; Kroon, J.; Looten, P.; Duflot, P.; Mathlouthi, M. *Carbohydr. Res.* **1999**, *322*, 274–278.
31. Kirschner, K. N.; Woods, R. J. *Proc. Natl. Acad. Sci. U.S.A.* **2001**, *98*, 10541–10545.
32. Rockwell, G. D.; Grindley, T. B. *J. Am. Chem. Soc.* **1998**, *120*, 10953–10963.